Chapter 6: DAMPED PHONONIC CRYSTALS AND ACOUSTIC METAMATERIALS

Mahmoud I. Hussein and Michael J. Frazier
Department of Aerospace Engineering Sciences,
University of Colorado Boulder, Boulder, CO 80309

The objective of this chapter is to introduce the topic of *damping* in the context of both its modeling and its effects in phononic crystals and acoustic metamaterials. First, we provide a brief discussion on the modeling of damping in structural dynamic systems in general with a focus on viscous and viscoelastic types of damping (Section 6.2), and follow with a non-exhaustive literature review of prior work that examined periodic phononic materials with damping (Section 6.3). In Section 6.4, we consider damped 1D diatomic phononic crystals and acoustic metamaterials as example problems (keeping our attention on 1D systems for ease of exposition as in previous chapters). We introduce the generalized form of Bloch theory, which is needed to account for both temporal and spatial attenuation of the elastic waves resulting from the presence of damping. We also describe the transformation of the governing equations of motion to a state-space representation to facilitate the treatment of the damping term that arises in the emerging eigenvalue problem. Finally, the effects of dissipation (based on the two types of damping models considered) on the frequency and damping ratio band structures are demonstrated by solving the equations developed for a particular choice of material parameters.

6.1 Introduction
6.2 Modeling of material damping
6.3 Elastic wave propagation in damped periodic media
6.4 Damped one-dimensional diatomic phononic crystal and acoustic metamaterial
6.4.1 Generalized Bloch theory and state-space transformation
6.4.1.1 Viscous damping
6.4.1.2 Viscoelastic damping
6.4.2 Damped Bragg scattering and local resonance
6.4.2.1 Viscous damping
6.4.2.2 Viscoelastic damping
6.5 References

6.1 Introduction

Damping is an innate property of materials and structures. Its consideration in the study of wave propagation is important because of its association with energy dissipation. We can concisely classify the sources of damping in phononic crystals and acoustic metamaterials into three categories, depending on the type and configuration of the unit cell. These are: (1) bulk material-level dissipation stemming from deformation processes (e.g., dissipation due to friction between internal crystal planes that slip past each other during deformation); (2) dissipation arising from the presence of interfaces or joints between different components (e.g., lattice structures consisting of interconnected beam elements [1]); and (3) dissipation associated with the presence of a fluid within the periodic structure or in contact with it. In general, the mechanical deformations that take place at the bulk material level, or similarly at interfaces or joints, involve microscopic processes that are not thermodynamically reversible [2]. These processes account for the dissipation of the oscillation energy in a manner that fundamentally alters the macroscopic dynamical characteristics including the shape of the frequency band structure. Similar yet qualitatively different effects occur due to viscous dissipation in the presence of a fluid. While the representation of the inertia and elastic properties of a vibrating structure is adequately accounted for by the usual "mass" and "stiffness" matrices, finding an appropriate damping model to describe observed experimental behavior can be a daunting task. This is primarily due to the difficulty in identifying which state variables the damping forces depend on and in formulating the best functional representation once a set of state variables is determined [3,4].

6.2 Modeling of material damping

Due to the diversity and complexity of dissipative mechanisms, the development of a universal damping model stands as a major challenge. A rather simple model proposed by Rayleigh [5] is the *viscous damping* model in which the instantaneous generalized velocities, $\dot{\mathbf{u}}$, are the only relevant state variables in the calculation of the damping force vector $\mathbf{f}_\mathrm{d}$ [4]. Using $\mathbf{C}$ to denote the damping matrix, this relationship is given by

$$\mathbf{f}_\mathrm{d}(t) = \mathbf{C}\dot{\mathbf{u}}(t). \tag{1}$$

While this description may be suitable when accounting for dissipation associated with the presence of a standard viscous medium (e.g., a Newtonian fluid), a physically realistic model of material damping will generally depend on a wider assortment of state variables. Such a model would represent nonviscous damping, of which *viscoelastic damping* is the most common type. In treating viscoelasticity, it is suitable to use Boltzmann's hereditary theory whereby the damping force depends upon the past history of motion via a convolution integral over a kernel function $\hbar(t)$:

$$\mathbf{f}_\mathrm{d}(t) = \mathbf{C}\int_0^t \hbar(t-\tau)\dot{\mathbf{u}}(\tau)d\tau. \tag{2}$$

The kernel function $\hbar(t)$ may take several forms, while recognizing that $\hbar(t-\tau) = \delta(t-\tau)$ recovers the familiar viscous damping model [4]. Fundamentally, any form is valid if it guarantees a positive rate of energy dissipation. Thus there are numerous possibilities. In Fig. 1, the Maxwell model for viscoelastic damping is illustrated; it consists of a linear spring and a viscous dashpot in a series configuration.

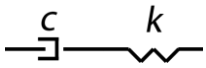

Figure 1: Maxwell model

The spring accounts for the fraction of mechanical energy that is stored during loading, while the viscous dashpot accounts for the remainder that is lost (not stored) from the system. The dashpot also adds a time dependence to the model as the rate of deformation becomes a factor. In this arrangement, the spring and dashpot experience the same axial force, $F = ku = c\dot{u}$. In addition, the total displacement has contributions from both elements, that is, $u = u_s + u_d$, where the subscripts s and d denote the spring and dashpot, respectively. Differentiating u with respect to time gives $\dot{u} = \dot{u}_s + \dot{u}_d$, which, by recalling the aforementioned equality of force within each element can be written in the following form:

$$\dot{u} = \frac{\dot{F}}{k} + \frac{F}{c}. \tag{3}$$

Assuming an initial displacement $u(0) = F(0)/k$ we can integrate equation (3) with respect to time to obtain the displacement function, $u(t)$. Corresponding to an elongation $u(t) = H(t)$, where $H(t)$ is the unit step-function, we obtain a relaxation response function, $F(t) = \hbar(t)$. Based on the Maxwell model of Fig. 1, the kernel function is [6]:

$$\hbar(t) = ke^{-\frac{k}{c}t}H(t) = \mu_1 e^{-\mu_2 t}H(t), \tag{4}$$

in which the constants $\mu_{1,2}$ (called relaxation parameters) may be determined from experiment. If the spring constant $k \to \infty$ in the Maxwell model, then elasticity, the mechanism of storing energy, is lost, and only the dissipative viscous mechanism remains. This is immediately apparent in equation (3) where $\dot{F}/k \to 0$ thus leading to the omission of the force-displacement relationship $F = ku$.

6.3 Elastic wave propagation in damped periodic media

There are several studies in the literature that consider the treatment of damping in the context of periodic phononic materials. Many of these focus on simulating finite periodic structures (e.g., Refs. [7-11]) which is different from carrying out a unit cell analysis. The latter approach has the advantage that it allows us to elucidate the broad effects of damping on the band structure characteristics. It is, therefore, more comprehensive because it provides information that can be relevant to a range of finite structure simulation scenarios.

In unit cell analysis, the dynamics of a periodic material, e.g., atomic-scale crystalline materials, phononic (or photonic) crystals, periodic acoustic (or electromagnetic) metamaterials, etc., is fully characterized by the application of Bloch theory [12] on a single representative unit cell. As discussed in earlier chapters, this theory states that the wave field in a periodic medium is also periodic, except that its periodicity is determined by the frequency versus wavevector dispersion relation. The form of the displacement response in a non-dissipative phononic material following Bloch theory is given by

$$\mathbf{u}(\mathbf{x}, \boldsymbol{\kappa}; t) = \tilde{\mathbf{u}}(\mathbf{x}, \boldsymbol{\kappa})e^{\mathbb{i}(\boldsymbol{\kappa}\cdot\mathbf{x}-\omega t)}, \tag{5}$$

where $\mathbf{u} = \{u_x, u_y, u_z\}$ is the displacement field, $\tilde{\mathbf{u}}$ is the displacement Bloch function, $\mathbf{x} = \{x, y, z\}$ is the position vector, $\boldsymbol{\kappa} = \{\kappa_x, \kappa_y, \kappa_z\}$ is the wavevector, $\mathbb{i} = \sqrt{-1}$, and ω and t denote temporal frequency and time, respectively.

Among the earlier studies that adopted a unit cell approach is the paper by Mead [13] which presented 1D discrete mass-spring-dashpot models and solved for the dispersion under structural damping (i.e., damping exhibiting velocity-independent forces). Similarly, Mikherjee and Lee [14], Castanier and Pierre [10], Zhang et al. [15] and Merheb et al. [16] provided dispersion relations using a complex elastic modulus (or a convolution integral expression in the case of Ref. [16]), and Langley [17] presented a corresponding analysis using a complex inertial term to account for the damping. In these studies, damping has therefore been incorporated in either the stiffness or mass matrix in the governing equations. Representing damping in the form of viscous or viscoelastic forces (as discussed in Section 6.2), on the other hand, is more realistic, but requires the incorporation of an additional state variable – velocity – in the governing equations of motion. Naturally this leads to an eigenvalue problem with a nontraditional format. Several studies considered this problem for different types of configurations (i.e., concerning the geometry, boundary conditions and constitutive material behavior), for example, Refs. [18,19].

A critical limitation to using equation (5) is that it assumes that a spatially propagating wave does not attenuate in time [20,21]. The allowance of a temporal loss factor was adopted by Mikherjee and Lee [14] in their investigation of a damped periodic composite (although limited to structural damping). In recent publications [22-24], the possibility of temporal attenuation has been incorporated in the Bloch formulation for viscous damping and it was shown that such treatment is consistent with results emanating from a free vibration analysis of corresponding finite periodic structures (whose theory of damping is well established [4]). It was observed that the band gaps in the damped unit cell dispersion match with the damped natural frequency gaps in the finite periodic structures only when the temporal component of Bloch theory is generalized to include a complex root λ, that is,

$$\mathbf{u}(\mathbf{x}, \boldsymbol{\kappa}; t) = \tilde{\mathbf{u}}(\mathbf{x}, \boldsymbol{\kappa}) e^{\mathbb{i}(\boldsymbol{\kappa}\cdot\mathbf{x})} e^{\lambda t}. \tag{6}$$

Here it should be noted that for the undamped case, $\lambda = \mathbb{i}\omega$ and equation (5) is recovered. While this form was successfully applied in Refs. [22-24], the models considered were limited to simple Kelvin-Voigt viscous damping models. In the next section, we present the formulations for analyzing damped one-dimensional diatomic phononic crystals and acoustic metamaterials on the basis of generalized Bloch theory, and for both viscous and viscoelastic damping as described in Section 6.2.

6.4 Damped one-dimensional diatomic phononic crystals and acoustic metamaterials

By considering lumped masses, springs, and damping elements, in this section we construct a simple ID model of a damped diatomic phononic crystal (represented by a "mass-and-mass" configuration as shown in Fig. 2a) and similarly a simple ID model of a damped diatomic acoustic metamaterial (represented by a "mass-in-mass" configuration as shown in Fig. 2b).

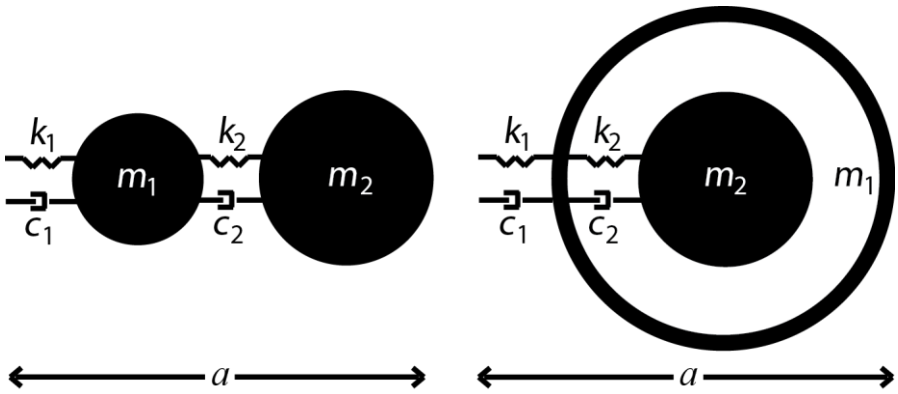

Figure 2: Lumped parameter unit cell model of (a) phononic crystal (mass-and-mass), and (b) acoustic metamaterial (mass-in-mass)

Considering unit cell periodicity, the set of homogeneous equations describing the motion of each mass in the phononic crystal model is obtained as follows [23]:

$$m_1\ddot{u}_1^j + (c_1+c_2)\dot{u}_1^j - c_2\dot{u}_2^j - c_1\dot{u}_2^{j-1} + (k_1+k_2)u_1^j - k_2u_2^j - k_1u_2^{j-1} = 0, \tag{7}$$

$$m_2\ddot{u}_2^j + (c_1+c_2)\dot{u}_2^j - c_2\dot{u}_1^j - c_1\dot{u}_1^{j+1} + (k_1+k_2)u_2^j - k_2u_1^j - k_1u_1^{j+1} = 0, \tag{8}$$

where u_α^j is the displacement of mass α in an arbitrary jth unit cell. In general, a unit cell and its neighbors may be identified by $j+n$, where $n = 0, -1, 1$ denote the present, previous, and subsequent unit cells, respectively. Similarly for the acoustic metamaterial model, the equations of motion corresponding to the two masses are [24]:

$$m_1\ddot{u}_1^j + c_1\left(2\dot{u}_1^j - \dot{u}_1^{j-1} - \dot{u}_1^{j+1}\right) + c_2\left(\dot{u}_1^j - \dot{u}_2^j\right) + k_1\left(2u_1^j - u_1^{j-1} - u_1^{j+1}\right) + k_2\left(u_1^j - u_2^j\right) = 0, \tag{9}$$

$$m_2\ddot{u}_2^j + k_2\left(u_2^j - u_1^j\right) + c_2\left(\dot{u}_2^j - \dot{u}_1^j\right) = 0. \tag{10}$$

6.4.1 Generalized Bloch theory and state-space transformation

Generalized Bloch theory

Writing the generalized Bloch theory of equation (6) in discrete format for the models shown in Fig. 2 involves the product of the spatial function $A_\alpha(x,\kappa) = \widetilde{U}_\alpha e^{\mathbb{i}(\kappa x + n\kappa a)}$ and a temporal function, which takes the form of $B(t,\lambda) = e^{\lambda t}$. Here, $\widetilde{U}_\alpha$ represent the complex wave amplitude, the variable a denotes the lattice constant, and $\kappa = \kappa_x$ for brevity. Thus the displacement function of mass α in the $(j+n)$th unit cell is given by

$$u_\alpha^{j+n}(x,\kappa;t) = A_\alpha(x,\kappa)B(t,\lambda) = \widetilde{U}_\alpha e^{\mathbb{i}(\kappa x + n\kappa a)+\lambda t}, \tag{11}$$

If we apply this form of the Bloch wave solution to equations (7) and (8) for the phononic crystal, we obtain a complex eigenvalue problem:

$$\lambda^2 m_1\widetilde{U}_1 + \lambda(c_1+c_2)\widetilde{U}_1 - \lambda c_2\widetilde{U}_2 - \lambda c_1\widetilde{U}_2 e^{-\mathbb{i}\kappa a} + (k_1+k_2)\widetilde{U}_1 - k_2\widetilde{U}_2 - k_1\widetilde{U}_2 e^{-\mathbb{i}\kappa a} = 0, \tag{12a}$$

$$\lambda^2 m_2\widetilde{U}_2 + \lambda(c_1+c_2)\widetilde{U}_2 - \lambda c_2\widetilde{U}_1 - \lambda c_1\widetilde{U}_1 e^{\mathbb{i}\kappa a} + (k_1+k_2)\widetilde{U}_2 - k_2\widetilde{U}_1 - k_1\widetilde{U}_1 e^{\mathbb{i}\kappa a} = 0, \tag{12b}$$

which in matrix form is represented as

$$\begin{bmatrix} \lambda^2 m_1 + \lambda(c_1 + c_2) + k_1 + k_2 & -\lambda\left(c_1 e^{-\mathbb{i}\kappa a} + c_2\right) - \left(e^{-\mathbb{i}\kappa a} k_1 + k_2\right) \\ -\lambda\left(c_1 e^{\mathbb{i}\kappa a} + c_2\right) - \left(e^{\mathbb{i}\kappa a} k_1 + k_2\right) & \lambda^2 m_2 + \lambda(c_1 + c_2) + k_1 + k_2 \end{bmatrix} \begin{bmatrix} \widetilde{U}_1 \\ \widetilde{U}_2 \end{bmatrix} = \begin{bmatrix} 0 \\ 0 \end{bmatrix}. \tag{12c}$$

Equation (12c) can be segregated in the following manner:

$$[\lambda^2 \mathbf{M} + \lambda \mathbf{C}(\kappa) + \mathbf{K}(\kappa)]\widetilde{\mathbf{U}} = \mathbf{0}. \tag{13}$$

Thus we identify the mass matrix **M**, damping matrix $\mathbf{C}(\kappa)$, and stiffness matrix $\mathbf{K}(\kappa)$ as:

$$\mathbf{M} = \begin{bmatrix} m_1 & 0 \\ 0 & m_2 \end{bmatrix}, \tag{14}$$

$$\mathbf{C}(\kappa) = \begin{bmatrix} c_1 + c_2 & -\left(c_1 e^{-\mathbb{i}\kappa a} + c_2\right) \\ -\left(c_1 e^{\mathbb{i}\kappa a} + c_2\right) & c_1 + c_2 \end{bmatrix}, \tag{15}$$

$$\mathbf{K}(\kappa) = \begin{bmatrix} k_1 + k_2 & -\left(k_1 e^{-\mathbb{i}\kappa a} + k_2\right) \\ -\left(k_1 e^{\mathbb{i}\kappa a} + k_2\right) & k_1 + k_2 \end{bmatrix}. \tag{16}$$

Applying equation (11) to equations (9) and (10) for the acoustic metamaterial yields the following complex eigenvalue problem:

$$\lambda^2 m_1 \widetilde{U}_1 + 2\lambda c_1(1 - \cos\kappa a)\widetilde{U}_1 + \lambda c_2\left(\widetilde{U}_1 - \widetilde{U}_2\right) + 2k_1(1 - \cos\kappa a)\widetilde{U}_1 + k_2\left(\widetilde{U}_1 - \widetilde{U}_2\right) = 0, \tag{17a}$$

$$\lambda^2 m_2 \widetilde{U}_2 + \lambda c_2\left(\widetilde{U}_2 - \widetilde{U}_1\right) + k_2\left(\widetilde{U}_2 - \widetilde{U}_1\right) = 0, \tag{17b}$$

which in matrix form can be represented as

$$\begin{bmatrix} \lambda^2 m_1 + 2\lambda c_1(1 - \cos\kappa a) + \lambda c_2 + 2k_1(1 - \cos\kappa a) + k_2 & -(\lambda c_2 + k_2) \\ -(k_2 + \lambda c_2) & \lambda^2 m_2 + \lambda c_2 + k_2 \end{bmatrix} \begin{bmatrix} \widetilde{U}_1 \\ \widetilde{U}_2 \end{bmatrix} = \begin{bmatrix} 0 \\ 0 \end{bmatrix}. \tag{17c}$$

Again, by segregating the coefficients, the damping and stiffness matrices can be identified and written as follows:

$$\mathbf{C}(\kappa) = \begin{bmatrix} 2c_1(1 - \cos\kappa a) + c_2 & -c_2 \\ -c_2 & c_2 \end{bmatrix}, \tag{18}$$

$$\mathbf{K}(\kappa) = \begin{bmatrix} 2k_1(1 - \cos\kappa a) + k_2 & -k_2 \\ -k_2 & k_2 \end{bmatrix}. \tag{19}$$

The acoustic metamaterial possesses the same mass matrix as the phononic crystal, given in equation (14). Finally, if we define the set of material parameters r_m, r_c, and r_k as follows:

$$r_m = m_2/m_1, \qquad r_c = c_2/c_1, \qquad r_k = k_2/k_1, \tag{20}$$

then we may write the system matrices for each of the two models in a more convenient form. Thus the system matrices for the phononic crystal become:

$$\mathbf{M} = m_2 \begin{bmatrix} 1/r_m & 0 \\ 0 & 1 \end{bmatrix} = m_2 \mathbf{M}_r, \tag{21}$$

$$\mathbf{C}(\kappa) = c_2 \begin{bmatrix} 1 + 1/r_c & -\left(1 + e^{-\mathbb{i}\kappa a}/r_c\right) \\ -\left(1 + e^{\mathbb{i}\kappa a}/r_c\right) & 1 + 1/r_c \end{bmatrix} = c_2 \mathbf{C}_r, \tag{22}$$

$$\mathbf{K}(\kappa) = k_2 \begin{bmatrix} 1 + 1/r_k & -\left(1 + e^{-\mathbb{i}\kappa a}/r_k\right) \\ -\left(1 + e^{\mathbb{i}\kappa a}/r_k\right) & 1 + 1/r_k \end{bmatrix} = k_2 \mathbf{K}_r, \tag{23}$$

and for the acoustic metamaterial,

$$\mathbf{C}(\kappa) = c_2 \begin{bmatrix} 2(1 - \cos \kappa a)/r_c + 1 & -1 \\ -1 & 1 \end{bmatrix} = c_2 \mathbf{C}_r, \tag{24}$$

$$\mathbf{K}(\kappa) = k_2 \begin{bmatrix} 2(1 - \cos \kappa a)/r_k + 1 & -1 \\ -1 & 1 \end{bmatrix} k_2 \mathbf{K}_r. \tag{25}$$

It should be noted that in general the matrices $\mathbf{C}_r$ and $\mathbf{K}_r$ are unitary matrices.

State-space transformation

For general damping, viscous or nonviscous, the equations of motion cannot be uncoupled by using an alternate set of coordinates (as done, for example, in Ref. [22] which treated proportional Rayleigh damping using Bloch modal analysis). To determine the complex eigenvalues, λ_s, $s = 1,2$, we develop a Bloch state-space formulation for each of the damping types. The formulation is based on a transformation of variables of the form:

$$\tilde{\mathbf{Y}} = \begin{bmatrix} \dot{\tilde{\mathbf{U}}} \\ \tilde{\mathbf{U}} \end{bmatrix}, \tag{26}$$

where the dot represents differentiation with respect to time.

6.4.1.1 Viscous damping

For general viscous damping, the Block state-space formulation is as follows [23]:

$$\begin{bmatrix} \mathbf{0} & m_2 \mathbf{M}_r \\ m_2 \mathbf{M}_r & c_2 \mathbf{C}_r(\kappa) \end{bmatrix} \dot{\tilde{\mathbf{Y}}} + \begin{bmatrix} -m_2 \mathbf{M}_r & \mathbf{0} \\ \mathbf{0} & k_2 \mathbf{K}_r(\kappa) \end{bmatrix} \tilde{\mathbf{Y}} = \mathbf{0}. \tag{27}$$

Now we write the solution as $\tilde{\mathbf{Y}} = \bar{\mathbf{Y}} e^{\lambda t}$. It is at this point that we introduce, for convenience, two additional material parameters, $\bar{\omega} = \sqrt{k_2/m_2}$ and $\beta = c_2/m_2$:

$$\left(\begin{bmatrix} \mathbf{0} & \mathbf{M}_r \\ \mathbf{M}_r & \beta \mathbf{C}_r(\kappa) \end{bmatrix} \lambda + \begin{bmatrix} -\mathbf{M}_r & \mathbf{0} \\ \mathbf{0} & \bar{\omega}^2 \mathbf{K}_r(\kappa) \end{bmatrix} \right) \bar{\mathbf{Y}} = \mathbf{0}. \tag{28}$$

Equation (28), which is a first order representation of the original second order eigenvalue problem, has two complex conjugate pairs of eigenvalues λ and eigenvectors $\bar{\mathbf{Y}}$. Given their orthogonality with respect to the system matrices, the eigenvectors decouple the equations into four modal equations with complex roots λ_{s^*}, $s^* = 1, \ldots, 4$ appearing in complex conjugate pairs and thus effectively representing two single-degree of freedom systems. Thus we can write:

$$\lambda_s = -\xi_s \omega_s \pm \mathbb{i} \omega_{d_s} = -\xi_s \omega_s \pm \mathbb{i} \omega_s \sqrt{1 - \xi_s^2}, \quad s = 1,2. \tag{29}$$

If we focus our attention on only the first eigenvalue in each complex conjugate pair, then we extract the damped natural frequency as:

$$\omega_{d_s}(\kappa) = \mathrm{Im}[\lambda_s(\kappa)], \quad s = 1,2, \tag{30}$$

and the corresponding damping ratio:

$$\xi_s(\kappa) = -\frac{\mathrm{Re}[\lambda_s(\kappa)]}{\mathrm{Abs}[\lambda_s(\kappa)]}. \quad s = 1,2. \tag{31}$$

6.4.1.2 Viscoelastic damping

In this section, we apply the Bloch state-space approach to the viscoelastic case by introducing a set of internal variables. We develop the state-space matrices using an approach proposed by Wagner and Adhikari [25] for finite structural dynamics systems, and then extend the analysis to the unit cell problem. The approach is specific to the case in which the constants $\mu_{1,2}$ in equation (4) are equal (i.e., $\mu = \mu_1 = \mu_2$).

According to Ref. [25], we define an internal variable $\mathbf{y}(t)$ as follows:

$$\mathbf{y}(t) = \int_0^t \mu e^{-\mu(t-\tau)}\, \dot{\mathbf{U}}(\tau) d\tau. \tag{32}$$

The Leibniz integral rule gives a formula for differentiation of a definite integral whose limits are functions of the differential variable:

$$\frac{\partial}{\partial t}\int_{a(t)}^{b(t)} f(x,t)\, dt = \int_{a(t)}^{b(t)} \frac{\partial}{\partial t} f(x,t)\, dt + f[b(t),t] \cdot \frac{\partial}{\partial t} b(t) - f[a(t),t]\frac{\partial}{\partial t} a(t). \tag{33}$$

Applying this rule to equation (32), we obtain:

$$\dot{\mathbf{y}}(t) = \int_0^t -\mu^2 e^{-\mu(t-\tau)}\, \dot{\mathbf{U}}(\tau) d\tau + \mu \dot{\mathbf{U}}(t) = \mu[\dot{\mathbf{U}}(t) - \mathbf{y}(t)]. \tag{34}$$

We may rewrite equation (34) as:

$$\dot{\mathbf{y}}(t) + \mu \mathbf{y}(t) = \mu \dot{\mathbf{U}}(t). \tag{35}$$

According to equations (2) and (4), the system of equations for a finite, viscoelastically damped system is

$$\mathbf{M}\ddot{\mathbf{U}}(t) + \mathbf{C}\int_0^t \mu e^{-\mu(t-\tau)} \dot{\mathbf{U}}(\tau) d\tau + \mathbf{K}\mathbf{U}(t) = \mathbf{f}(t). \tag{36}$$

However, for our unit cell Bloch wave propagation problem, for which the damping and stiffness matrices are wavenumber-dependent and $\mathbf{f}(t) = \mathbf{0}$, we get:

$$\mathbf{M}_r\ddot{\mathbf{U}} + \beta \mathbf{C}_r(\kappa) \int_0^t \mu e^{-\mu(t-\tau)} \dot{\mathbf{U}}(\tau) d\tau + \bar{\omega}^2 \mathbf{K}_r(\kappa)\mathbf{U} = \mathbf{0}. \tag{37}$$

With equation (32), this becomes:

$$\mathbf{M}_r\ddot{\mathbf{U}} + \beta \mathbf{C}_r(\kappa)\mathbf{y} + \bar{\omega}^2 \mathbf{K}_r(\kappa)\mathbf{U} = \mathbf{0}. \tag{38}$$

Next, we solve for $\mathbf{y}$ in equation (35) and substitute the result into equation (38):

$$\mathbf{M}_r\ddot{\mathbf{U}} + \beta \mathbf{C}_r(\kappa)\left[\dot{\mathbf{U}} - \frac{1}{\mu}\dot{\mathbf{y}}\right] + \bar{\omega}^2 \mathbf{K}_r(\kappa)\mathbf{U} = \mathbf{0}. \tag{39}$$

At this point, incorporating equation (39) into a state-space matrix equation format will result in non-square matrices. To produce square and block-symmetric state-space matrices, we formulate another equation. Premultiplying equation (35) by $\mathbf{C}_r(\kappa)$ and dividing by μ^2 yields:

$$-\frac{1}{\mu}\mathbf{C}_r(\kappa)\dot{\mathbf{U}} + \frac{1}{\mu^2}\mathbf{C}_r(\kappa)\dot{\mathbf{y}} + \frac{1}{\mu}\mathbf{C}_r(\kappa)\mathbf{y} = \mathbf{0}. \tag{40}$$

In first order state-space form, equations (39) and (40) become:

$$\begin{bmatrix} \mathbf{0} & \mathbf{M}_r & \mathbf{0} \\ \mathbf{M}_r & \beta\mathbf{C}_r(\kappa) & -\frac{\beta}{\mu}\mathbf{C}_r(\kappa) \\ \mathbf{0} & -\frac{\beta}{\mu}\mathbf{C}_r(\kappa) & \frac{\beta}{\mu^2}\mathbf{C}_r(\kappa) \end{bmatrix} \dot{\tilde{\mathbf{Z}}} + \begin{bmatrix} -\mathbf{M}_r & \mathbf{0} & \mathbf{0} \\ \mathbf{0} & \bar{\omega}^2\mathbf{K}_r(\kappa) & \mathbf{0} \\ \mathbf{0} & \mathbf{0} & \frac{\beta}{\mu}\mathbf{C}_r(\kappa) \end{bmatrix} \tilde{\mathbf{Z}} = \mathbf{0}, \tag{41}$$

where $\tilde{\mathbf{Z}} = [\dot{\mathbf{U}} \quad \mathbf{U} \quad \mathbf{y}]^{\mathsf{T}}$. We assume the solution $\tilde{\mathbf{Z}} = \bar{\mathbf{Z}}e^{\lambda t}$, and subsequently develop the eigenvalue problem:

$$\left(\begin{bmatrix} \mathbf{0} & \mathbf{M}_r & \mathbf{0} \\ \mathbf{M}_r & \beta\mathbf{C}_r(\kappa) & -\frac{\beta}{\mu}\mathbf{C}_r(\kappa) \\ \mathbf{0} & -\frac{\beta}{\mu}\mathbf{C}_r(\kappa) & \frac{\beta}{\mu^2}\mathbf{C}_r(\kappa) \end{bmatrix} \lambda + \begin{bmatrix} -\mathbf{M}_r & \mathbf{0} & \mathbf{0} \\ \mathbf{0} & \bar{\omega}^2\mathbf{K}_r(\kappa) & \mathbf{0} \\ \mathbf{0} & \mathbf{0} & \frac{\beta}{\mu}\mathbf{C}_r(\kappa) \end{bmatrix} \right) \bar{\mathbf{Z}} = \mathbf{0}. \tag{42}$$

Upon obtaining the eigenvalues λ_{s^*}, now mathematically a set of six values, $s^* = 1, \ldots, 6$, we can extract the two complex conjugate pair values (remaining two roots are spurious) that physically represent the modes of damped wave propagation, exactly as defined in equations (30) and (31).

As implied in the above formulation, and supported by the definition of the Maxwell element (Fig. 1 and equation (3)), in the limit $\mu \to \infty$, the viscous Bloch state-space formulation of equation (28) is recovered. That is, high values of μ represent more viscous behavior (less dependence on the past history), while low values of μ represent more viscoelastic behavior (more dependence on the past history).

6.4.2 Damped Bragg scattering and local resonance

For both the phononic crystal and the acoustic metamaterial models in Fig. 2, we generate dispersion curves using for demonstration a specific set of material parameters: $r_m = 9$, $r_c = 0.5$, $r_k = 1$, and $\bar{\omega} = 149.07\,\text{rad/s}$. The parameter β is varied to show the dependence on the damping intensity. In Figs. 3-6, plots corresponding to the phononic crystal (mass-and-mass model) appear on the left while those pertaining to the acoustic metamaterial (mass-in-mass model) appear on the right. While these results are dependent on values chosen for the parameters r_m, r_c and r_k, they provide some basic insight on the effects of damping on the behavior of phononic crystals and acoustic metamaterials.

6.4.2.1 Viscous damping

Here we show the frequency (Fig. 3) and damping ratio (Fig. 4) band structures for the case of viscous damping, obtained by solving equation (28). We observe in Fig. 3 that as the damping intensity $\beta/\bar{\omega}$ is increased, the optical branch for both the phononic crystal and the acoustic metamaterial drops while the acoustic branch experiences little change – this in turn leads to a reduction in the size of the band gap. For the phononic crystal, the descent of the optical branch takes place at slightly faster rates at low wavenumbers compared to high wavenumbers; whereas for the acoustic metamaterial significantly higher drop rates take place at high wavenumbers compared to low wavenumbers. The damping ratio diagram in Fig. 4 follows a corresponding trend with an indication that the effect of damping is slightly more significant at low wavenumbers for the phononic crystal and noticeably more significant at high

wavenumbers for the acoustic metamaterial. We also observe that at low wavenumbers the damping ratio values for the phononic crystal exceed those of the acoustic metamaterial for a given damping intensity $\beta/\bar{\omega}$, and vice versa at high wavenumbers. With regards to the damping ratios of the acoustic branch modes, these are higher for the phononic crystal compared to the acoustic metamaterial.

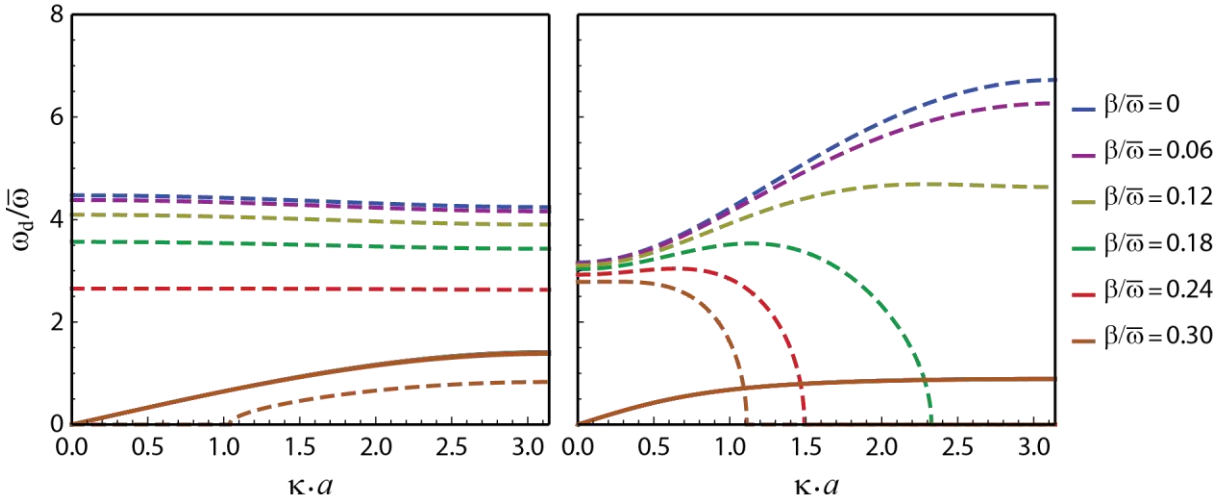

Figure 3: Frequency band structure for viscous damping case:
phononic crystal (left) and acoustic metamaterial (right)

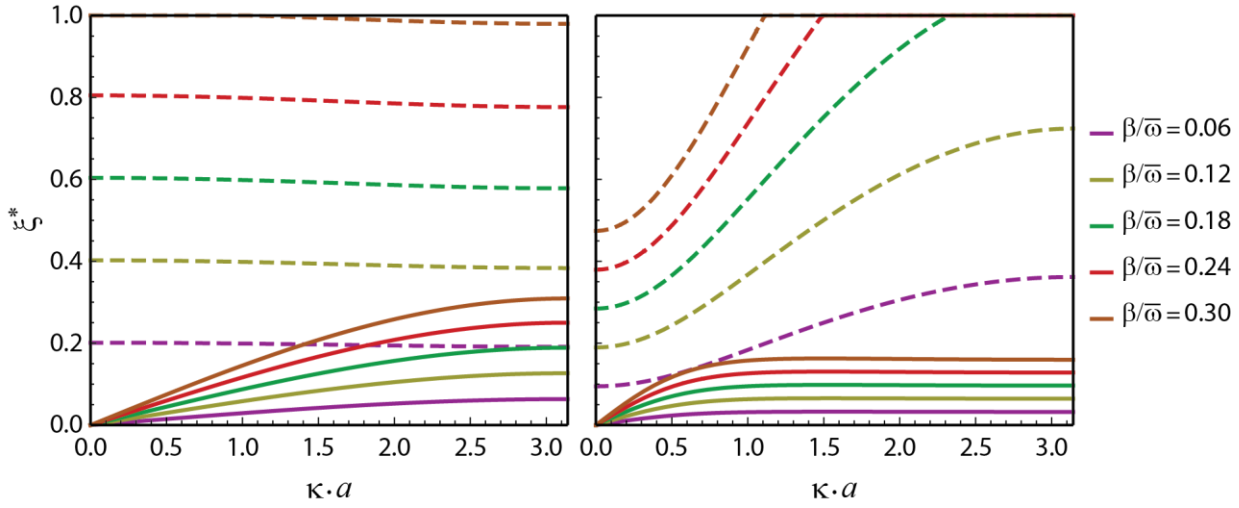

Figure 4: Damping ratio band structure for viscous damping case:
phononic crystal (left) and acoustic metamaterial (right)

6.4.2.2 Viscoelastic damping

As noted in Section 6.4.1.2, when $\mu > 0$, viscoelastic behavior is better represented by "low" μ and, in contrast, viscous behavior is better represented by "high" μ. What qualifies as a low/high value of μ depends on the other parameters in the damping matrix $\mathbf{C}(\kappa)$. If μ is such that $\frac{1}{\mu}\mathbf{C}(\kappa) \approx \mathbf{0}$ compared to

$\mathbf{C}(\kappa)$ (i.e., $\mathbf{C}(\kappa) + \frac{1}{\mu}\mathbf{C}(\kappa) \approx \mathbf{C}(\kappa)$), then dominantly viscous behavior can be expected. For our model, we find $\mu = 10^8$ reflects viscous behavior well. To represent the viscoelastic behavior, we set $\mu = 10^3$ and show the solution of equation (42) in Figs. 5 and 6.

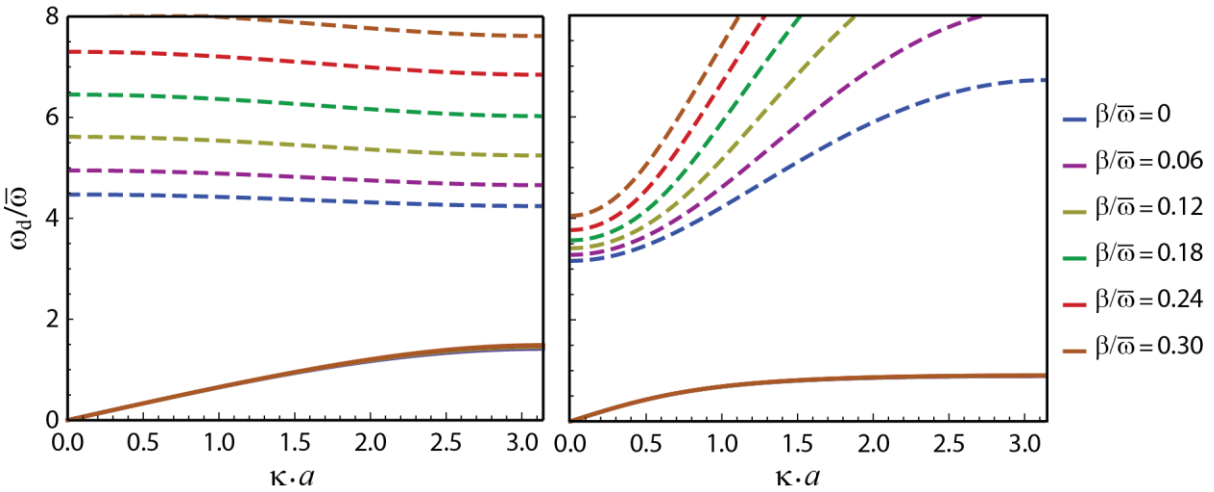

Figure 5: Frequency band structure for viscoelastic damping case: phononic crystal (left) and acoustic metamaterial (right)

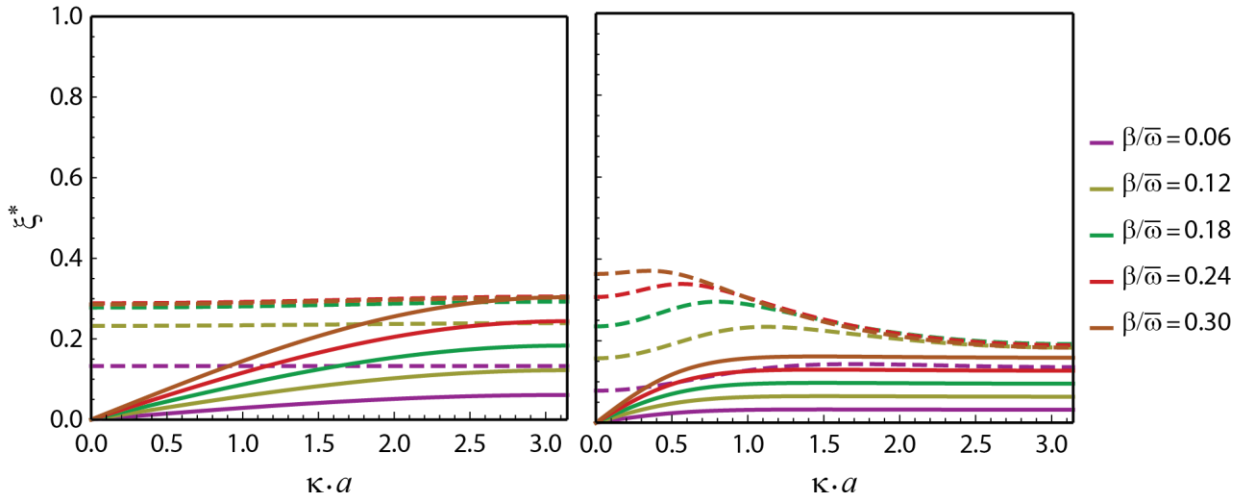

Figure 6: Damping ratio band structure for viscoelastic damping case: phononic crystal (left) and acoustic metamaterial (right)

Unlike the viscous damping case, we notice that in this model of viscoelastic damping, the optical dispersion branches for both the phononic crystal and the acoustic metamaterial rise with the damping intensity. Subsequently, this increases the size of the band gap – a desirable feature for many applications such as vibration isolation and frequency sensing. The sensitivity of the changes in the optical branches again seems to be highest in the acoustic metamaterial at high wavenumbers. The damping ratio band structures shown in Fig. 6 indicate less sensitivity overall to damping intensity

compared to the viscous damping case. This is because a portion of the energy associated with the viscoelastic forces is stored in the spring element (as discussed in Section 6.2) and not dissipated.

We recall that both the phononic crystal and acoustic metamaterial models considered are based on the same ratios of mass, stiffness and damping (see Fig. 2 and equation 20). Yet, the effects of damping are different. This is a manifestation of the fundamental difference in the wave propagation mechanism of Bragg scattering (that takes place in phononic crystals) and that of local resonance (that takes place in acoustic metamaterials).

6.5 References

1. A. S. Phani, J. Woodhouse and N. A. Fleck, "Wave Propagation in Two-dimensional Periodic Lattices," J. Acoust. Soc. Am. 119, 1995-2005 (2006).
2. A. S. Nowick and B. S. Berry, "Anelastic Relaxation in Crystalline Solids," New York: Academic Press 1972.
3. C. W. Bert, "Material Damping: An Introductory Review of Mathematic Measures and Experimental Techniques," J. Sound Vib. 29, 129-153 (1973).
4. J. Woodhouse, "Linear Damping Models for Structural Vibration," J. Sound Vib. 215, 547-569 (1998).
5. J. W. S. Rayleigh, "Theory of Sound," London: MaCmillon and Co. 1878.
6. Y. C. Fung and P. Tong, P., "Classical and Computational Solid Mechanics," World Scientific Publishing Co. 2001.
7. Y. Yong and Y. K. Lin, "Propagation of Decaying Waves in Periodic and Piecewise Periodic Structures of Finite Length," J. Sound Vib. 129, 99-118 (1989).
8. I. E. Psarobas, "Viscoelastic Response of Sonic Band-gap Materials," Phys. Rev. B 64, 012303 (2001).
9. P. W. Mauriz and M. S. Vasconcelos and E. L. Albuquerque, "Acoustic Phonon Power Spectra in a Periodic Superlattice," Phys. Status Solidi *B* 243, 1205-1211 (2006).
10. M. P. Castanier and C. Pierre, "Individual and Interactive Mechanisms for Localization and Dissipation in a Mono-coupled Nearly-periodic Structure," J. Sound Vib. 168, 479-505 (1993).
11. Y. Liu, D. Yu, H. Zhao, J. Wen and X. Wen, "Theoretical Study of 2D PC with Viscoelasticity Based on Fractional Derivative Models," J. Phys. D Appl. Phys. 41, 065503 (2008)
12. F. Bloch, "Über die Quantenmechanik der Electron in Kristallgittern," Z. Phys. 52, 555–600 (1928).
13. D. J. Mead, "A General Theory of Harmonic Wave Propagation in Linear Periodic Systems with Multiple Coupling," J. Sound Vib. 27, 235-260 (1973).
14. S. Mukherjee and E. H. Lee, "Dispersion Relations and Mode Shapes for Waves in Laminated Viscoelastic Composites by Finite Difference Methods.," Comput. Struct. 5, 279-285 (1975).
15. X. Zhang, Z. Liu, J. Mei and Y. Liu, "Acoustic Band Gaps for a 2D Periodic Array of Solid Cylinders in Viscous Liquid," J. Phys.-Condens. Mat. 15, 8207-8212 (2003).
16. B. Merheb, P. A. Deymier, M. Jain, M. Aloshyna-Lesuffleur, S. Mohanty, A. Baker and R. W. Greger, "Elastic and Viscoelastic Effects in Rubber-air Acoustic Band Gap Structures: A Theoretical and Experimental Study," J. Appl. Phys. 104, 064913 (2008).
17. R. S. Langley, "On the Forced Response of One-dimensional Periodic Structures: Vibration Localization by Damping," J. Sound Vib. 178, 411-428 (1994).
18. E. Tassilly, "Propagation of Bending Waves in a Periodic Beam," Int. J. Eng. Sci. 25, 85-94 (1987).

19. R. Sprik and G. H. Wegdam, “Acoustic Band Gaps in Composites of Solids and Viscous Liquids,” Solid State Commun 106, 77-81 (1998).
20. R. P. Moiseyenko and V. Laude, “Material Loss Influence on the Complex Band Structure and Group Velocity in Phononic Crystals,” Phys. Rev. B 83, 064301 (2011).
21. F. Farzbod and M. J. Leamy, "Analysis of Bloch's Method in Structures with Energy Dissipation," Journal of Vibration and Acoustics, J. Vib. Acoust. 133, 051010 (2011).
22. M. I. Hussein, “Theory of Damped Bloch Waves in Elastic Media,” Phys. Rev. B 80, 212301 (2009).
23. M. I. Hussein and M. J. Frazier, ”Band Structures of Phononic Crystals with General Damping,” J. Appl. Phys. 108, 093506 (2010).
24. M. J. Frazier and M. I. Hussein, “Dissipative Effects in Acoustic Metamaterials,” *Proceedings of Phononics 2011*, Paper Phononics-2011-0172, pp. 84-85, Santa Fe, New Mexico, USA, May 29-June 2, 2011.
25. N. Wagner and S. Adhikari, S., “Symmetric State-Space Method for a Class of Nonviscously Damped Systems,” AIAA J. 41, 951-956 (2003).